
Cooperative binding of m-AMSA to nucleic acids

Rebecca H. Elmore, Randy M. Wadkins and David E. Graves*

Department of Chemistry, University of Mississippi, MS 38677, USA

Received June 8, 1988; Revised and Accepted September 12, 1988

ABSTRACT

The equilibrium binding of the antitumor agent m-AMSA (4'-(9-acridinylamino) methanesulfon-m-aniside) has been examined by optical methods. These studies which have focused on the low bound drug concentrations (r values < 0.02 , base pairs) reveal m-AMSA to bind calf thymus DNA in a highly cooperative manner as indicated by the initial positive slope of the Scatchard plot. In contrast, the studies on the parent 9-aminoacridine under identical conditions demonstrate that this compound binds DNA in a noncooperative (neighbor exclusion) manner. The positive cooperative binding phenomenon of m-AMSA is probed as a function of ionic concentration and shown to exist over the range of salt concentrations examined (0.01 to 0.1 M); however, the magnitude of the cooperative binding is altered. This observation of cooperativity is consistent with earlier studies on biologically active compounds and may be related to such binding parameters as binding sequence selectivity and/or structural perturbations to the DNA structure.

INTRODUCTION

m-AMSA (4'-(9-acridinylamino)methanesulfon-m-aniside) (NSC-249992) is a potent antitumor agent which was developed by Bruce Cain and coworkers in the early 1970s (1,2). This acridine analog has been shown to be highly effective against a variety of experimental tumors and leukemias. m-AMSA is used as a primary component of combination chemotherapy for the treatment of a variety of leukemias and lymphomas in Canada and Europe and is currently undergoing phase III clinical trials in the U.S. (3-5). The chemotherapeutic effectiveness of m-AMSA has generated considerable interest concerning the mechanism(s) of action of the drug as well as the biophysical parameters which influence its binding specificity and biological effectiveness.

The molecular mechanism(s) involved in the antineoplastic activities of m-AMSA is unknown. In the cell, the interactions of m-AMSA with nuclear DNA is believed to induce scission of the DNA by affecting the function of topoisomerases (6). Recently, Pommier and coworkers demonstrated m-AMSA to induce the formation of protein associated single strand breaks in nuclear DNA. Characterization of the role of m-AMSA in this action revealed that the drug was acting via inhibition of the topoisomerase II, presumably through formation of a ternary complex between the drug, topoisomerase II and the DNA (7,8). In addition, they demonstrated that the addition of m-AMSA results in the stimulation of covalent binding of the

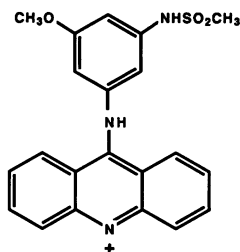


Figure 1. Chemical structure of m-AMSA, 4'-(9-acridinylamino)methanesulfon-m-anisidide, NSC-249992.

topoisomerase II to the DNA, with the concentrations of m-AMSA needed to observe this increased enzyme binding to DNA being relatively low (9). Thus, it was of particular interest to examine the DNA binding properties of m-AMSA at very low bound drug concentrations.

Recent studies examining the biophysical properties of selected antitumor agents suggest that several of these drugs may interact in a highly selective manner with nucleic acids and in fact may involve a small number of specific binding sites on the DNA. Observations of a positive cooperative binding phenomenon have been documented for several potent antitumor antibiotics including actinomycin (10); adriamycin and daunorubicin (11); the anthracenedione, mitoxantrone (DHAQ) (12); and the oligopeptides, netropsin and distamycin (13,14). In each case, a pronounced curvature of the binding isotherm (Scatchard Plot) was observed at low levels of bound drug, indicative of a positive cooperative binding process.

The antitumor activity and clinical usefulness of m-AMSA has prompted this laboratory to examine the binding of m-AMSA to nucleic acids under similar conditions which are conducive for positive cooperative binding to be observed (i.e., ionic strength and temperature). Under these conditions, the binding of m-AMSA to calf thymus DNA at low drug/DNA concentration ratios is shown to be highly cooperative. In contrast, under identical conditions, the parent compound, 9-aminoacridine, is shown to bind in a noncooperative manner to DNA.

Numerous studies have provided information concerning the binding of m-AMSA with nucleic acids. These studies have provided insight into its intercalative mode of binding, equilibrium binding affinities, site exclusion size, and base sequence preferences (15,16). However, due to experimental constraints, these binding studies have focused on relatively high concentrations of bound drug. This report describes the equilibrium binding properties of m-AMSA to nucleic acids with special emphasis on m-AMSA - DNA interactions at low concentrations of bound drug. In addition, the effects of ionic strength on the positive cooperative binding properties are examined. From this study, information concerning the phenomena of cooperative binding, preferential binding to certain sequences, and propagation of DNA structural perturbations is probed.

EXPERIMENTAL METHODS

Materials

m-AMSA Preparations. m-AMSA (NSC-249992) was a gift of Dr. Robert R. Engle, Chemical Resources Section of the National Cancer Institute. The purity of the m-AMSA was confirmed by TLC, using KC₁₈ Whatman plates and methylene chloride-methanol-H₂O (100:20:2) as the solvent. The m-AMSA showed marginal solubility in water, thus a stock solution was prepared by dissolving approximately 0.2 milligrams in neat dimethyl sulfoxide. This stock solution was then diluted 1:10 with sodium phosphate buffer, centrifuged for 5 minutes on an eppendorf microfuge and the clear supernatant stored in an eppendorf vial for the duration of the experiment at room temperature and protected from the light. Stock drug concentrations were determined by using a Varian Cary 2290 UV-visible spectrophotometer via Beer-Lambert analysis in the absence of DNA. A molar absorptivity value of $\epsilon_{436\text{nm}}=12000 \text{ M}^{-1}\text{cm}^{-1}$ (14) was used to determine the concentration of drug in the absence of DNA. All drug solutions were prepared fresh on the day of the experiment from dry material stored at -20°C.

DNA Preparations. Calf thymus DNA (type I) was purchased from Worthington Biochemicals and purified according to the method of Chaires (17). Briefly, the DNA was sheared by sonification for 30 minutes at 5°C in the presence of bubbling N₂. Subsequently, the DNA was subjected to T₁ RNase and Proteinase K (Boehringer Mannheim) digestions, followed by repeated extractions with a 1:1 mixture of chloroform and phenol and then precipitated with cold ethanol. The DNA pellet was then dissolved in sodium phosphate buffer, pH 7.0, 0.001 M disodium EDTA, and the appropriate sodium chloride concentration as determined by experimental protocol. After dialysis against the appropriate buffer, the DNA was filtered using 0.45 μ syringe filter (Millipore) prior to experimental use. The concentrations of the DNA solutions are stated in terms of base pairs (bp) using the molar absorptivity of $\epsilon_{260\text{nm}}=13,200 \text{ M}^{-1}\text{cm}^{-1}$. Purity and integrity of the DNA preparation was determined and checked routinely by monitoring the UV spectrum, and by gel electrophoresis.

Methods

Spectral Properties of m-AMSA. The interaction of m-AMSA with nucleic acids results in a marked change in the visible region of the drugs absorption spectrum as shown in Figure 2. This hypochromic effect can be utilized as a means to monitor the equilibrium binding of this drug to DNA. Assuming a two state system consisting of bound and free drug species, the absorbance at a particular given wavelength can represent contributions from both the free and bound drug species. The molar absorptivity of the bound species was determined by plotting the reciprocal change in absorbance versus the reciprocal of the DNA (base pair) concentration. The curve was extrapolated to infinite DNA concentration to determine ϵ_b . The molar absorptivity at 436 nm for m-AMSA bound to DNA was calculated to be $\epsilon_b=6900 \text{ M}^{-1}\text{cm}^{-1}$, thus $\Delta\epsilon = 5100 \text{ M}^{-1}\text{cm}^{-1}$.

Optical Titration. A DNA solution of known volume and concentration was added to the 10 cm reference and sample cells. Small aliquots of a known concentration of stock m-AMSA solution were titrated into the sample cell. After each addition, the solution was exhaustively mixed and allowed to re-equilibrate to the desired temperature. The temperature was maintained constant at 22.6°C using a Lauda constant temperature circulating bath. The absorbance was then determined directly from the CRT display of the Cary 2290 at selected wavelengths of maximum absorbance change (436nm) and the isosbestic wavelength (475 nm) using the statistical algorithm which signal averages 300 readings and provides the mean and standard deviation of the absorbances at the desired wavelengths. Free ligand concentrations were kept at less than 2×10^{-6} M due to the aggregation properties of this drug in aqueous solution as determined from Beer-Lambert titrations. From the change in absorbance of the m-AMSA as a result of its interaction with DNA it was possible to calculate the equilibrium binding constant, K_{int} , and the site exclusion parameter, n .

Analysis of Drug Binding. Data obtained by the optical titrations were plotted as r/C_f vs. r (18). Theoretical curves shown as the solid lines through the data points were "fit" using both the two-site (11,12) and allosteric (11,13,14, 19) binding models to quantitate the cooperative binding effect. Parameters used to fit these models to the binding data are provided in Table I.

The two-site model recognizes the heterogeneous population of binding sites within the DNA. According to this model, certain sites on the DNA may exhibit highly cooperative high affinity sites, while other sites may exist as noncooperative low affinity binding sites. Individual parameters for the two types of binding (cooperative and noncooperative) are determined by the McGhee and von Hippel equation (20). However, rather than using one calculation to fit the complete binding isotherm, the two-site model takes in to account both the cooperative and noncooperative binding sites. The subpopulations of binding sites are fit independently, then summed to provide the overall shape of the binding isotherm which is correlated to experimental data.

In addition, we have analyzed the positive cooperative binding of m-AMSA to calf thymus DNA using the model for induced allosteric changes in the DNA initially used by Crothers and coworkers to characterize the binding of distamycin and netropsin to calf thymus DNA (13,14). The allosteric binding model assumes two distinct structures of DNA, designated form I and form II. The equilibrium constant for the conversion of a base pair at the interface between the two forms is represented by the parameter S . Nucleation of one form within a region of the other form is represented by the equilibrium constant $\sigma^2 S$, where σ accounts for the difficulty in forming an interface between the two forms in a nucleation process. The binding characteristics of the ligand to the two forms are respectively described as K_1 and K_2 (the intrinsic binding constants) and n_1 and n_2 (the neighbor exclusion sizes) for both structures of DNA. Parameters used to fit the allosteric binding model to the data are provided in Table I.

Both the allosteric and the two-site binding analyses require an input of six or more para-

eters to define the respective models, and thus precludes the usefulness of a nonlinear regression analysis for determining the best fit for the binding parameters for either system. However, as a reference point for analyzing both systems, the binding curves were characterized at the higher r values (the portion of the binding curve exhibiting a negative slope) by the neighbor exclusion model

$$r/C_f = K(1-nr)((1-nr)/(1-(n-1)r))^{(n-1)}$$

where K_{int} is the intrinsic binding constant and n is the binding size exclusion parameter. Data were fit using in this manner with a nonlinear least squares fitting routine based on the Marquart-Levenberg algorithm. The binding constant and size exclusion parameters were then utilized as close approximations for the values of K_2 of the allosteric binding constant (binding of the drug to high affinity "Form 2" DNA) and the K_1 of the two-site model (binding to the highly cooperative DNA) as presented in Table I. The remaining parameters for both models were then estimated by iterative adjustments. Adjustments of plus or minus ten percent in the values obtained for the remaining fitting parameters did not significantly affect the theoretical binding isotherms.

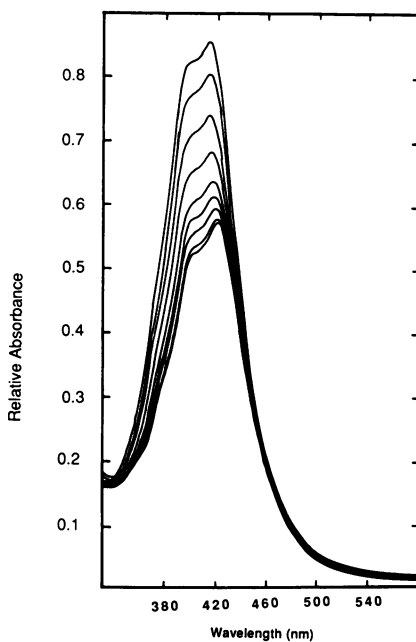


Figure 2. Representative absorption spectra resulting from the interaction of m-AMSA with calf thymus DNA. Both the drug and DNA were dissolved in 0.01 M sodium phosphate, pH 7.0, 0.001M disodium EDTA, 0.1 M sodium chloride. The sample was maintained at 22°C. The top spectrum represents free m-AMSA, while the remaining spectra result from serial additions of concentrated DNA.

TABLE 1. Equilibrium Binding Parameters for the Interaction of m-AMSA with Calf Thymus DNA as Derived from the Allosteric Binding Model of Crothers and coworkers (13,14)

[NaCl] M	$K_1(M^{-1})$	$K_2(M^{-1})$	K_2/K_1	τ_1	τ_2	n_1	n_2	S^a	σ^b
0.01	2.3×10^4	1.1×10^5	5	8	.95	6	4	.993	.0025
0.05	1.3×10^4	4.2×10^4	4	8	.95	6	6	.992	.0025
0.10	8.6×10^3	2.6×10^4	3	8	.95	7	6	.990	.0025

Equilibrium Binding Parameters for the Interaction of m-AMSA with Calf Thymus DNA as Derived from the Two-Site Model of Krugh and coworkers (11,12)

[NaCl] M	$K_1(M^{-1})$	$K_2(M^{-1})$	n_1	n_2	ω_1	ω_2	ratio
0.01	1.2×10^5	6.7×10^4	3	2.5	.99	50	35
0.05	4.1×10^4	3.2×10^4	4	3	.99	100	50
0.10	1.9×10^4	1.2×10^4	3	2.5	.99	70	35

^a S is defined as the equilibrium constant for the conversion of a base pair at the interface between form I and form II DNA. ^b The σ term is a reflection on the energy required to convert a base pair from form I to form II DNA. The overall equilibrium constant in the conversion of form I to form II DNA is $\sigma^2 S$.

RESULTS

Spectral Properties of the m-AMSA-DNA Complex

The interaction of m-AMSA with calf thymus DNA results in a marked change in the visible region of the drug absorption spectrum as shown in Figure 2. This hypochromic effect can be used to monitor the equilibrium binding of m-AMSA to DNA. In the free state, the absorption maximum of m-AMSA occurs at 434 nm. As DNA is added to the sample, the absorbance of the drug at 434 nm is shown to decrease. The absorbance of the drug when fully complexed to DNA is approximately 58 percent of the free drug absorbance. In addition, there is a slight bathochromic shift of 8 nm to 442 nm as the DNA concentration is increased to saturating levels. An isosbestic point is observed at 472 nm for the complex.

Cooperative Binding of m-AMSA to Nucleic Acids

The Scatchard plot representing the binding of m-AMSA to calf thymus DNA is presented in Figure 2. These data extend previously reported results of Wilson (15) and Waring (16) to very low r values ($r < 0.05$, in concentration of bound drug per base pair). Examination of the binding data at this low range of r values provides novel information concerning the binding of

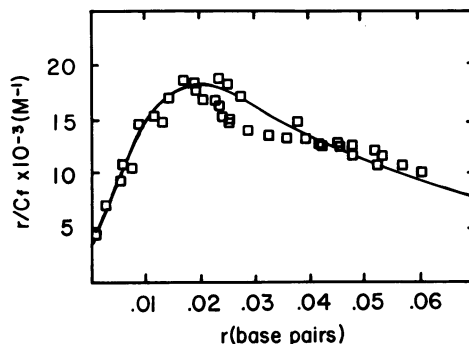


Figure 3. Scatchard plot for the binding of m-AMSA to calf thymus DNA. Data obtained by serial titration of drug into a known concentration of DNA and monitoring the change in the absorbance at 436 nm. This binding curve was generated in 0.01 M sodium phosphate, pH 7.0, 0.001 M disodium EDTA, 0.1 M sodium chloride. The temperature was maintained at 22.6°C with a circulating water bath (Lauda). Drug concentrations ranged from 0.1 to 1 micromolar, while the DNA ranged from 10 to 150 micromolar. The smooth line drawn through the data points represents calculated binding isotherms using the two-site model of Krugh and coworkers (11). Parameters used to fit this model to the experimental data are provided in Table I.

m-AMSA to DNA. These data reveal that m-AMSA binds to calf thymus DNA in a highly cooperative manner, as indicated by the initial positive slope of the Scatchard plot at the lower range of r values. This positive portion of the binding curve reaches a maximum r/C_f value at an r of 0.02 which corresponds to one drug bound per 50 base pairs. At values of r which are greater than 0.02, the binding curve exhibits a negative slope which is consistent with the McGhee and von Hippel neighbor exclusion model for drug binding (20).

The smooth curve drawn through the experimental data represents a best-fit using both the allosteric binding model of Crothers and coworkers (13,14) and the two-site model of Krugh (11,12). Parameters used to fit these theoretical curves are presented in Table I. At r values which are greater than 0.02 (in the region of the binding curve exhibiting the negative slope), the McGhee and von Hippel neighbor exclusion binding model can be used to determine both the intrinsic binding constant, K_{int} , and the site exclusion size, n . Treatment of this portion of the binding curve with the neighbor exclusion model allowed values for K_{int} of $3.18 \times 10^4 M^{-1}$ and a binding site size exclusion parameter of 3.2 base pairs per bound drug to be determined. These values are in good agreement with earlier studies by Wilson and Waring (15,16).

This positive cooperativity appears to be a unique binding phenomenon for the m-AMSA analog in comparison to other acridine compounds. The binding of the parent 9-aminoacridine to calf thymus DNA is shown the scatchard plot in Figure 4. This binding study was performed under identical conditions (i.e., ionic strength, drug and DNA concentrations, and temperature) as the previously described for the m-AMSA binding study shown in Figure 3.

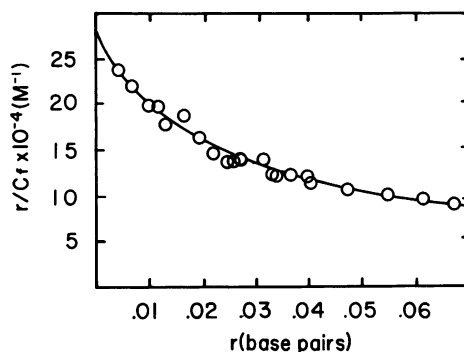


Figure 4. Scatchard plot for the equilibrium binding of 9-aminoacridine to calf thymus DNA. Binding data were obtained under conditions as described in the legend of Figure 3. The smooth line drawn through this data represents the best fit using the neighbor exclusion model (20).

Clearly, the 9-aminoacridine is shown to bind in a non-cooperative manner as indicated by the negative slope of the binding isotherm over the complete range of r values which were examined. The smooth line drawn through these data were generated from the McGhee and von Hippel equation, and the intrinsic association constant was calculated to be $2.2 \times 10^5 \text{ M}^{-1}$. Although the 9-aminoacridine demonstrates a 10-fold higher affinity for binding to DNA as compared to m-AMSA, it is relatively ineffective as an antitumor agent. Over the range of bound drug concentrations ($r < 0.02$) where positive cooperativity was observed for m-AMSA binding to calf thymus DNA, there was no evidence of any positive cooperative binding be-

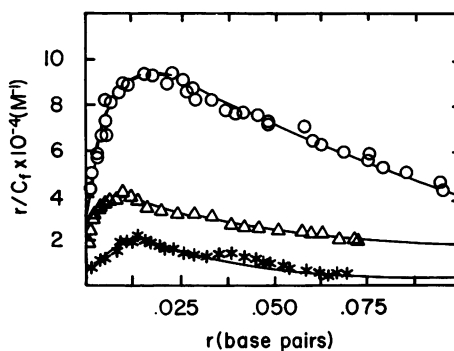


Figure 5. Scatchard analysis showing the effects of varying the salt concentration on the binding properties of m-AMSA to calf thymus DNA. Data represented by open circles (O-O) corresponds to low salt experiment (0.01 M sodium chloride); the open triangles (Δ - Δ) correspond to the intermediate salt concentration of 0.05 M sodium chloride; and the asterisks (*-*) corresponds to 0.1 M sodium chloride. Binding isotherms were obtained by titration methods as described in the legend of Figure 3.

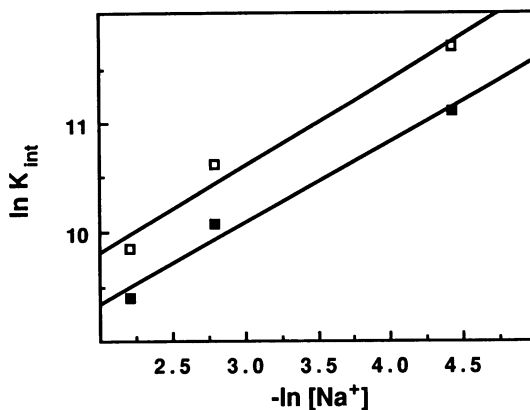


Figure 6. A plot of the log K versus the negative log of the sodium ion concentration for the binding of m-AMSA to calf thymus DNA. The open circles (O-O) and open squares (°-°) represent K_1 and K_2 , respectively, as calculated from the two-site model as shown in Table I.

havior in the binding of the parent 9-aminoacridine to calf thymus DNA. Rather, the negative slope is indicative of a neighbor exclusion model for the drug-DNA interaction.

Effects of Ionic Strength on the Cooperative Binding of m-AMSA to DNA

Of particular importance in this study was to determine the effects of ionic strength on the cooperative binding phenomenon observed for the interaction of m-AMSA with calf thymus DNA. As observed in Figure 5, m-AMSA is shown to bind to calf thymus DNA in a highly cooperative manner under a variety of salt conditions, ranging from very low ionic strengths (0.01 M) to moderate ionic strengths (0.1 M). From these studies, the degree of cooperativity as indicated by the initial positive slope of the binding isotherm appears to be greatest at the lower ionic strengths (0.01 M - 0.05 M). As the ionic strength is increased, the initial positive slope of the binding curve decreases, along with the magnitude of the maximum r/C_f value. The binding experiments characterizing the influence of ionic effects on the cooperative binding phenomenon were limited to salt concentrations between 0.01 to 0.1 M. Accurate binding isotherms at the lower range of r values could not be obtained at higher ionic strengths due to solubility properties of the m-AMSA.

The best fits through these data are represented by the solid lines, which were generated using the two-site model. Parameters used to fit this model to the data are provided in Table I. As would be expected for the interaction of a charged ligand to DNA the binding affinities, K_1 and K_2 , corresponding to the intrinsic binding constants for sites 1 and 2, decrease as a function of increasing ionic strength. Interestingly, the ω_1 cooperativity parameter is shown to be relatively insensitive to the ionic strength of the solution, with ω_1 values ranging from 50 to 70 in going from the most cooperative low salt condition to the less cooperative high salt concentration of 0.1 M.

Using the K_1 and K_2 values which were generated from the computer fits of these binding isotherms, the Manning-Record theory of ion condensation can be used to examine the number of counter ions released at both sites on the DNA upon binding m-AMSA (21-22). In Figure 6, the natural log of K_1 and K_2 are plotted as a function of the negative natural log of the sodium ion concentrations. Slopes corresponding to $-m\psi$ of 0.75 for site I and 0.80 for site II were calculated. From these slopes, the number of counterions released upon binding the m-AMSA to both the cooperative sites (type I sites) and noncooperative sites (type II sites) can be calculated using the modified ion-condensation theory of Wilson and Lopp (23) which takes into account the effects of intercalation of the drug between adjacent base pairs of the DNA on the release of counterions from the DNA duplex. From these data, we calculate that 1.1 and 1.2 counterions are released upon binding m-AMSA to type I (cooperative sites) and type II (non-cooperative sites), respectively. These data indicate that a single charge is carried on the m-AMSA which binds to either of the types of binding sites on the DNA.

DISCUSSION

The binding of m-AMSA to DNA is via intercalation of its acridine ring system between the adjacent base pairs of the duplex DNA (24). This intercalative binding process has been the subject of numerous investigations over the last decade resulting in information concerning the binding affinities, base sequence selectivities, and binding site size. The antitumor activity of m-AMSA is presumed to be mediated by this DNA binding and recently has been shown to be associated with protein mediated single strand breaks via a ternary complex between the m-AMSA, topoisomerase II, and DNA (5-8).

The present studies provide a unique insight into the interactions of m-AMSA with nucleic acids. This study extends previously reported binding isotherms to much lower r values and reveal that at low bound drug concentrations ($r < 0.02$), m-AMSA binds DNA in a positive cooperative manner, as indicated by the concave-downward Scatchard plots shown in Figures 2 and 4. In addition, the DNA binding properties of m-AMSA were compared to those of the parent compound 9-aminoacridine under identical conditions. In contrast, at low r values where positive cooperative binding was observed for the interaction of m-AMSA with DNA, the parent 9-aminoacridine was shown to exhibit a negative cooperativity. These results imply that the presence of the bulky methanesulfon-m-anisidide at the N9 position on the acridine ring may be responsible for influencing this specific binding phenomenon.

This positive cooperative binding phenomenon has been observed for a number of DNA binding drugs including adriamycin, daunorubicin, actinomycin D, mitoxantrone, distamycin, and netropsin (10-14). In addition to these antitumor antibiotics, other compounds reporting positive cooperative binding in their equilibrium mode of DNA binding are the carcinogens HAAF, NQO (10), and aflatoxin B₁ (25).

The cooperative binding of m-AMSA to DNA was demonstrated to be influenced by the

ionic strength of the reaction solution. The results observed for the m-AMSA binding isotherms are similar to the results obtained in earlier binding studies with the antitumor drugs actinomycin D and mitoxantrone (10,12). The degree of cooperativity (as indicated by the steepness of the humped region of the Scatchard plot) appears to increase at low ionic strengths (0.01 M sodium chloride). As the ionic strength is increased, the initial positive slope of the Scatchard plot is decreased. In addition, the positive cooperative binding of distamycin and netropsin to DNA appear to be relatively insensitive to the ionic concentration (13,14). In contrast, the cooperative binding observed with the binding of adriamycin and daunorubicin to calf thymus DNA is highly dependent on the ionic concentration (11). The positive cooperative binding for these compounds with DNA was observed only at moderate ionic strengths (0.1 - 0.2 M). At low and high salt concentrations (0.01 and 0.1 M, respectively), the positive cooperative binding phenomenon was not observed. The significance of the positive cooperative binding phenomenon is as yet unknown, along with the physical chemical properties which dictate this particular binding property to m-AMSA. These studies demonstrate the effects of ionic concentration on both the binding affinities and positive cooperative binding phenomenon observed for the of m-AMSA with calf thymus DNA. As expected from the binding of a charged ligand to DNA, the highest binding affinity is observed at low ionic strength. The displacement of sodium ion by the drug may be accomplished more efficiently at lower ionic strengths than at higher sodium concentrations. In comparing the binding properties of m-AMSA with other drugs such as adriamycin and daunorubicin, one can speculate on the origin of cooperative binding for both types of drugs. The positive charge on the m-AMSA is located on the region of the molecule which intercalates between the adjacent base pairs of duplex DNA, while adriamycin and daunorubicin both carry a positive charge on the amino sugar side-chain portion of the molecule. Thus, the effects of ionic strength on the cooperative binding process of these compounds could be dramatically different, with the cooperative binding of the anthracyclines being highly influenced by the concentration of counterions associated with the sugar phosphate backbone of the duplex DNA (association of the positively charged side chain with the minor grooves of the DNA) and m-AMSA being less dependent, due to insertion of the charged acridine ring between the adjacent base pairs of the DNA. Thus it is apparent that the charge distribution and DNA helix flexibility play a major role in the cooperative binding process of antitumor agents to DNA.

The data from this study were analyzed by two different methods. Parameters used to fit these models to the experimental data are provided in Table I. The two-site model allows for the existence of high affinity sites based not only on regional DNA structure, but also possibly occurring as a result of particular base sequences (and resulting structural conformations induced by these sequences), tertiary structures such as supercoils, cruciforms, and localized regions of non "B" form DNA. The degree of cooperativity using this model is readily apparent through a comparison of the cooperativity parameter, ω . At 0.1 M sodium chloride con-

centration, the ω for the cooperative binding sites is 70, while the noncooperative binding sites show a ω value of 0.98, indicative of negative cooperativity. In an analysis of the parameters used to generate this visual fit, we find that saturation of the site I regions of the DNA occurs at an r value of .009, corresponding to one drug bound per 110 base pairs, thus providing an indication that the size of these highly cooperative binding sites is quite small (< 1%) relative to the remainder of the DNA lattice. A comparison of the cooperativity parameters obtained in the salt dependence study reveals that ω is relatively insensitive to the ionic strength within this range of ionic concentrations. In addition, the saturation size of site I regions did not change as a function of the ionic concentration.

An alternative method used to examine the positive cooperative binding of ligands to DNA is the allosteric model which was proposed by Crothers and coworkers (13,14). According to this model, two structurally different forms of DNA may exist. Binding of a ligand to form I DNA results in a conformational or allosteric change in the DNA structure to form II which exhibits a greater affinity for binding the ligand than form I. As ligands are bound to the form I DNA (as indicated by the positive slope of the scatchard curve), the form I DNA is induced to undergo this allosteric transition to the higher affinity conformation, form II, until all of the form I DNA has been converted to the form II conformation, hence the r/C_f maxima. At this point, the DNA is totally in form II, and the neighbor exclusion model is obeyed for filling the remaining binding sites. The binding characteristics of the ligand to the two forms are respectively described as K_1 and K_2 (the intrinsic binding constants) and n_1 and n_2 (the neighbor exclusion sizes) for both structures of DNA. The degree of cooperativity is measured by the K_2/K_1 ratio given by the term XQ in Table I.

In the case of the binding isotherm obtained at 0.1 M sodium chloride concentration, the site exclusion parameters were calculated to be one drug bound per 6 base pairs for both forms of DNA. The cooperativity index (ratio of the intrinsic binding constants of Form 1 and Form 2) is equal to 3. At an r value of 0.02, corresponding to the site on the binding curve where r/C_f reaches a maximum value, the calculated allosteric binding isotherm predicts that 95 % of the form I DNA has been converted to form II.

Studies thus far have been unable to elucidate which model best describes the positive cooperative binding of ligands to DNA. From these studies, it is obvious that both models are consistent with the experimental data. Further studies are underway to provide a basis for determining the molecular interactions that give rise to this cooperative binding phenomenon. Both the two-site and allosteric models provide plausible explanations which may be used to describe this cooperativity in terms of the existence of high affinity or cluster sites on the DNA and/or the effects of DNA structure on selected drug binding.

ACKNOWLEDGEMENTS

This work was supported by funding from the National Cancer Institute, CA-41474, the Petroleum Research Fund of the American Chemical Society #17692-G4, and the Cottrell Research Corporation.

*To whom correspondence should be addressed

REFERENCES

1. Cain, B., Atwell, G. and Denny, W. (1975) *Journal of Medicinal Chemistry* 18, 1110-1117.
2. Denny, W.A., Baugley, B.C., Cain, B.F., and Waring, M.J. (1983) in "Molecular Aspects of Anti-Cancer Drug Action", Neidle, S. and Waring, M.J., Eds., Springer Verlag, Weinheim, 1-34.
3. Marsoni, S. and Wittes, R. (1984) *Cancer Treatment Reports* 68, 77-84.
4. Legha, S.S., Gutterman, J.U., Hall, S.W., Benjamin, R.S., Burgess, M.A., Valdivieso, M. and Bodey, G.P. (1978) *Cancer Research* 38, 3712-3716.
5. Winton, E.F., Hearn, E.B., Vogler, W.R., Johnson, L., Logan, T. and Raney, M. (1983) *Cancer Treatment Reports* 67, 977-980.
6. Ross, W.E., Glaubiger, D.L. and Kohn, K.W. (1979) *Biochim. Biophys. Acta* 562, 41-50.
7. Pommier, Y., Mattern, M.R., Schwartz, R.E., Zwelling, L.A. and Kohn, K.W. (1984) *Biochemistry* 23, 2927-2932.
8. Minford, J., Pommier, Y., Filipinski, J., Kohn, K.W., Kerrigan, D., Mattern, M., Michaels, S., Schwartz, R. and Zwelling, L.A. (1986) *Biochemistry* 25, 9-16.
9. Pommier, Y., Covey, J.M., Kerrigan, D., Markovits, J. and Pham, R. (1987) *Nucleic Acids Research* 15, 6713-6731.
10. Winkle, S.A. and Krugh, T.R. (1982) *Nucleic Acids Research* 9, 3175-3186.
11. Graves, D.E. and Krugh, T.R. (1983) *Biochemistry* 22, 3941-3947.
12. Rosenberg, L.S., Carvlin, M.J. and Krugh, T.R. (1986) *Biochemistry* 25, 1002-1008.
13. Dattagupta, N., Hogan, M. and Crothers, D.M. (1980) *Biochemistry* 19, 5998-6005.
14. Dattagupta, N., Hogan, M. and Crothers, D.M. (1981) *Biochemistry* 20, 1438-1445.
15. Wilson, W., Baguley, B., Wakelin, L. and Waring, M. (1981) *Molecular Pharmacology* 20, 404-414.
16. Waring, M. (1976) *European Journal of Cancer* 12, 995-1001.
17. Chaires, J.B., Dattagupta, N. and Crothers, D.M. (1982) *Biochemistry* 21, 3933-3940.
18. Scatchard, G. (1949) *Annals New York Academy Science* 51, 660-672.
19. Walker, G.T., Stone, M.P. and Krugh, T.R. (1985) *Biochemistry* 24, 7462-7471.
20. McGhee J.D. and von Hippel, P.H. (1974) *Journal of Molecular Biology* 86, 469-489.
21. Record, M.T., Jr., Anderson, C.F. and Lohman, T.M. (1978) *Quarterly Review of Biophysics* 11, 103-178.
22. Manning, G.S. (1978) *Quarterly Review of Biophysics* 11, 179-246.
23. Wilson, W.D. and Lopp, I.G. (1979) *Biopolymers* 18, 3025-3041.
24. Feigon, J., Denny, W., Leupin, W. and Kearns, D.R. (1984) *Journal of Medicinal Chemistry* 27, 450-465.
25. Stone, M.P., Gopalakrishnan, S., Harris, T.M. and Graves, D.E. (1988) *Journal of Biomolecular Structure and Dynamics* 5, 1025-1041.